

Quasinormal modes and thermodynamic properties of GUP-corrected Schwarzschild black hole surrounded by quintessence

Ronit Karmakar ^{*}, Dhruba Jyoti Gogoi [†] and Umananda Dev Goswami [‡]
Department of Physics, Dibrugarh University, Dibrugarh 786004, Assam, India

We study the Quasinormal Modes (QNMs) of the Schwarzschild black hole surrounded by a quintessence field after implementing the quantum corrections to its solution as required by the Generalized Uncertainty Principle (GUP). We analyze the dependence of the QNMs on the deformation parameters of GUP as well as on the quintessence parameter. For better accuracy, we compare the results of the QNMs obtained via Mashhoon method with the semi-analytical WKB method. Further, we study the thermodynamic properties of the GUP-corrected Schwarzschild black hole and check for any dependence with the deformation parameters and the quintessence parameter. In particular, we compute the Hawking temperature, heat capacity and entropy for the black hole and analyze the results graphically to show the dependency of the thermodynamic properties on the deformation parameters as well as the quintessence parameter. Black hole remnant has been studied and it is shown that the possible existence of remnant radius as well as remnant temperature depends on the deformations introduced. However, it is observed that the GUP-corrected black hole constructed here can not become a remnant. Black hole shadow has been investigated and it was found that the shadow has linear relations with the model parameters. We conclude the work with a summary note and future possibilities.

PACS numbers:

Keywords: Quasinormal Modes; Black holes; Gravitational Waves; Generalized Uncertainty Principle

I. INTRODUCTION

Black holes and Gravitational Waves (GWs) are two of the most fascinating predictions of General Relativity (GR). Black holes are among the most mysterious objects in our universe that have attracted the attention of scientific community for many decades. It is widely believed that when a sufficiently massive star runs out of fuel, the inward pull of gravity becomes dominant and there is a rapid collapse of matter towards the centre, which ultimately results in the formation of a black hole. A black hole interacts with its surrounding matter and is generally in a perturbed state. Such perturbations cause the black hole to undergo oscillation and that leads to the emission of GWs [1–5]. GWs are ripples in the spacetime fabric, generated by accelerating massive objects, which propagate at the speed of light. The LIGO-Virgo collaboration declared the first-ever detection of GWs on 14th of september 2015 [6], almost after 100 years of their prediction by prominent physicist A. Einstein in 1916. Since then, a number of detections of GWs has been reported by the collaboration [7–10]. It has generated a new era of gravitational astronomy, the likes of which has never been seen before.

Quasinormal Modes (QNMs) are some complex frequencies associated with the GWs that represent the reaction of a black hole, after some perturbations act on it [2, 3, 11–17]. There are different methods of calculations of QNMs from the black holes [2]. One of the simplest and elegant methods of finding out the QNMs was devised by B. Mashhoon, which is commonly called as the Mashhoon Method [2, 11, 18–20]. It is an analytical method which is easy to handle for a simple system. The most frequently used and trusted method of QNM analysis is the Wentzel-Kramers-Brillouin (WKB) method [2, 3, 21], which was initially utilized by Schutz and Will [22]. Improvements were made in this method by Konoplya who introduced corrections in WKB calculations upto 6th orders [14]. Recently, more higher order corrections are introduced in this method ([23] and references therein). In this work we consider both these methods of analyzing the QNMs for the sake of accuracy in the calculation. Apart from these, numerous works have been done on the analytical and numerical techniques to calculate the QNMs associated with the black hole perturbations in recent times [24–31]. Other works related to black hole physics may be found in [32, 33] and in the references therein.

Recently, the black hole physics and related thermodynamics have also attracted researcher's attention and a lot of such works can be seen in recent times in literature [34–44]. It was after the ground-breaking works of Bekenstein and Hawking that cemented the idea of interpreting the black hole as a thermodynamic system, showing the corresponding properties like temperature and entropy. Hawking proposed that a black hole emits radiation from its event horizon [45–47] and Bekenstein showed that as the black hole engulfs matter, the information associated with it is not lost but is incorporated in the horizon area

^{*}Email: ronit.karmakar622@gmail.com

[†]Email: moloydhruba@yahoo.in

[‡]Email: umananda2@gmail.com

of the black hole [48–50]. These ideas led to a revolution in black hole thermodynamics.

The discovery of Riess and Perlmutter, which showed that the universe is expanding with an acceleration [51, 52] led to a flood of theoretical models coming forward to resolve this unexpected observation. In the majority of such models the idea of dark energy was invoked to interpret this colossal expansion (see [53] for a review). One of the convenient ideas to deal with it was the Λ CDM model, in which Einstein’s cosmological constant was reintroduced as a homogeneous and isotropic fluid with the negative pressure and is considered to be the cause of this present state of expansion of the universe [54]. The cosmological constant was thought to originate out of quantum fluctuations of vacuum, but its theoretically predicted value could not match the observational value. To alleviate this problem, dynamical scalar field models were proposed, and the most common among them is the quintessence model of dark energy. In this model a scalar field minimally coupled to gravity is used to describe this late time accelerated expansion. Detailed about and current status of the quintessence model can be seen in Refs. [53–59].

Many works can be found in literature where the black hole thermodynamics is studied with a surrounding field. In 2003, a Schwarzschild black hole surrounded by a quintessence was studied and corresponding thermodynamic properties were examined by Kiselev [60]. He showed that presence of the surrounding field has a major impact on the properties of a black hole. Subsequently, Chen *et al.* [61] considered a d -dimensional black hole with a quintessence matter surrounding it and examined thermodynamic properties of the black hole. Reissner-Nordström black holes were examined with a quintessential surrounding by Wei and Chu [62]. Thermodynamics of Narai type black holes were considered by Fernando with a quintessential surrounding [63]. Recently, it is seen that many research works have considered the effects of quantum corrections via the Generalized Uncertainty Principle (GUP) on the thermodynamics of black hole [64–66]. One such work was carried out by Shahjalal in 2019 [64], where he compared the effects of the quantum deformations with and without the presence of quintessential surroundings. The case of rotating non-linear magnetically charged black holes was taken up by Ndongmo *et al.* [67], in which thermodynamics of the black hole was studied. Moreover, Anacleto *et al.* [65] studied the quantum-corrected Schwarzschild black holes and analyzed the absorption and scattering processes. González *et al.* [68] studied a 3-dimensional Godel black hole and calculated the QNMs and Hawking radiation. Further, Lütüoglu *et al.* [66] studied the thermodynamics of Schwarzschild black holes with the quintessential surrounding and GUP. They showed that the upper and lower bounds on various functions like temperature and entropy depend on the deformation parameters as well as on the quintessence coefficient, and also presented plots of P-V isotherms.

The study of black hole shadows has also been carried out in recent times as they provide useful insights into the black hole event horizon as well as into the optical properties of a black hole [69, 70]. The initial work in this direction was done by Sygne [71] and Luminet [72] in the 1970s and for rotating Kerr black holes by Bardeen [73]. Lately, an interesting work on QNMs and shadows of Schwarzschild black hole was performed by Anacleto *et al.* [74], where they considered the GUP-modified Schwarzschild black hole solutions and calculated the QNMs and shadows of the black holes, and showed the dependency of these properties on the deformation parameters. In recent times, many works have been done in this field [75–81].

Thus, inspired from the ongoing endeavours to explore these novel ideas, in this work we intend to study the various properties of a GUP-corrected Schwarzschild black hole surrounded by a quintessence field, such as the QNMs and thermodynamic properties like Hawking temperature, entropy, heat capacity and surface gravity. To the best of our information, GUP with both linear and quadratic terms has not been incorporated to Schwarzschild black hole surrounded by quintessence. The novelty of GUP that it introduces a minimum length scale, that is the Planck’s length, might play an important role in the properties of black holes [66, 74]. Also, we plan to analyse the possibility of association of the parameters of our model with the shadow radius of the black hole.

The rest of the paper is organized as follows. In section II, we compute the QNMs of the GUP-corrected Schwarzschild black hole surrounded by a quintessence field using the Mashhoon method and the semi-analytical WKB method, and analyze the results. In section III, we study the thermodynamic properties of the black hole and present a graphical analysis of dependency of the thermodynamic properties on the deformation parameters as well as on the quintessence coefficient. Then we analyze the black hole shadow with respect to variations in the model parameters. We summarize our results and present some concluding remarks in section IV.

II. QUASINORMAL MODES OF A GUP-CORRECTED SCHWARZSCHILD BLACK HOLE

The general form of the black hole metric as initially derived by Kiselev [60], in which he considered a Schwarzschild black hole surrounded by a quintessence dark energy with a particular energy density, can be expressed by

$$ds^2 = -g(r) dt^2 + \frac{1}{g(r)} dr^2 + r^2 d\Omega^2, \quad (1)$$

where $d\Omega^2 = d\theta^2 + \sin^2 \theta d\phi^2$ and the metric function $g(r)$ has the form:

$$g(r) = 1 - \frac{2M}{r} - \frac{e}{r^{3\omega+1}}. \quad (2)$$

In this function M is the mass of the black hole, ω is the equation of state parameter of the quintessence field, and e is the positive normalization coefficient that is dependent on the quintessence density. Since the recent past, a quantum correction to various black hole solutions, including the Schwarzschild one has been introduced via GUP in order to avoid singularities in such solutions by introducing a minimum length other than zero [82]. Under this correction, the normal metric of a black hole is modified, which gives a corresponding new horizon of the black hole. Thus, for example, in the case of Schwarzschild black hole, the original Schwarzschild horizon radius r_h of the black hole has to be replaced with the GUP-corrected radius r_{hGUP} for this purpose [74]. The basic steps of incorporation of GUP correction into the black hole metric (1) are the following.

Considering the modified Heisenburg algebra, we may write

$$\Delta x \Delta p \geq \frac{\hbar}{2} \left(1 - \frac{\alpha l_p}{\hbar} \Delta p + \frac{\beta l_p^2}{\hbar^2} (\Delta p)^2 \right), \quad (3)$$

where α and β are two dimensionless deformation parameters, and l_p is the Planck's length. Taking the unit system with $G = c = \hbar = l_p = 1$, equation (3) can be solved for Δp , which gives

$$\Delta p \approx \frac{4r_h + \alpha}{2\beta} \left[1 - \sqrt{1 - \frac{4\beta}{(4r_h + \alpha)^2}} \right]. \quad (4)$$

Here the uncertainty in position is taken as the horizon diameter $2r_h$ and we end up with the following expression [65]:

$$E_{GUP} \geq E \left[1 - \frac{4\alpha}{r_h} + \frac{16\beta}{r_h^2} + \dots \right], \quad (5)$$

where E_{GUP} is the GUP-corrected energy of the black hole. Now considering the assumption that $E \sim M$, $E_{GUP} \sim M_{GUP}$ and calculating $r_h = \frac{2M}{1-e}$ from the function (2), we obtained the relation,

$$M_{GUP} \geq M \left[1 - \frac{4\alpha}{r_h} + \frac{16\beta}{r_h^2} \right] = M \left(1 - \frac{2\alpha(1-e)}{M} + \frac{4\beta(1-e)^2}{M^2} \right). \quad (6)$$

Thus, finally the line element of a GUP-corrected Schwarzschild black hole surrounded by a quintessence field ($\omega = -1/3$) takes the form:

$$ds^2 = -f(r)dt^2 + \frac{1}{f(r)}dr^2 + r^2d\Omega^2 \quad (7)$$

with the modified metric function

$$f(r) = 1 - \frac{2M}{r} \left(1 - \frac{2\alpha(1-e)}{M} + \frac{4\beta(1-e)^2}{M^2} \right) - e \equiv 1 - \frac{2M_{GUP}}{r} - e. \quad (8)$$

This metric function gives the GUP-corrected horizon radius as $r_{hGUP} = 2M_{GUP}/(1-e)$. Fig. 1 shows the behaviours of the original metric and the GUP-corrected metric as functions of r for various values of the related parameters. From the figure it is seen that there is only one event horizon for the black hole for different values of the parameters. There is no other horizon obtained for the black hole. The left plot shows that with the increasing values of α , the horizon radius becomes smaller. Whereas the middle and the right plots show that with the increasing β and e values respectively, the horizon radius increases. It is also seen that the effect of parameter β is more dominant than that of the parameters α and e .

At this stage it is necessary to mention that the small values of the GUP parameters is an obvious choice because any correction term that we introduce into our theory cannot be larger than the base term involved as these corrections are generally very minute in nature. In the literature, we found that the values of these parameters have been considered less than unity [64, 66, 74, 83]. This choice is well motivated as we are considering only small corrections to the original uncertainty relation and it is demanded for the derivation of the metric expression. Similarly, the quintessence parameter (e) has been constrained for the case of a Schwarzschild black hole surrounded by a quintessence field in Ref. [84], where the authors found a bound on the quintessential parameter as $10^{-21} \leq eM \leq 10^{-11}$. On the other hand in Refs. [61, 85], it can be seen that the quintessential parameter is taken of the order ~ 0.1 . So, in our study we consider reasonably small values of these parameters.

A. QNMs by Mashhoon Method

Mashhoon method is an analytical method of calculating the QNMs of a black hole by comparing its effective potential with a standard potential, such as the Poschl-Teller potential [18] or the Eckart potential [11]. Starting from the metric function $f(r)$,

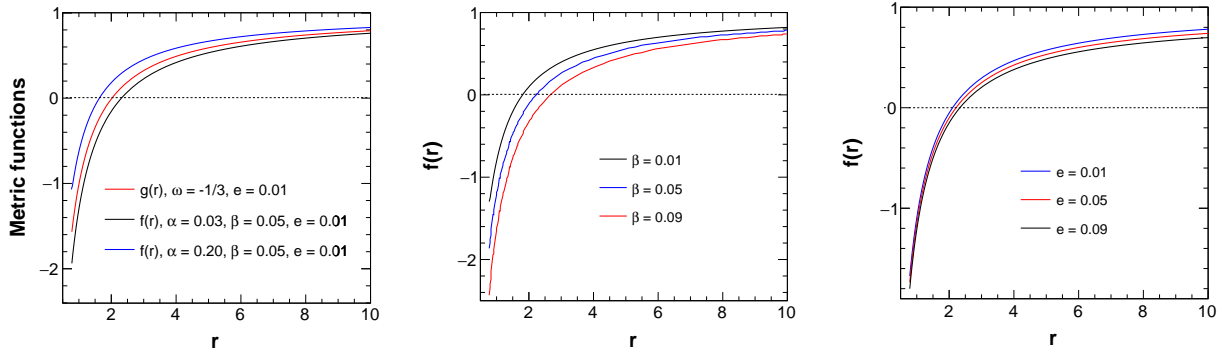


FIG. 1: Behaviours of the original metric and the GUP-modified metric as a function of r for different values of the associated parameters as shown. In the middle plot $\alpha = 0.09$ is used, whereas in the right plot $\alpha = \beta = 0.02$ is used. In all the three plots $M = 1$ is used. This value of M is used for all plots and analysis of this work, if otherwise not stated.

the effective black hole potential can be obtained from the formula [16, 23]:

$$V_l(r) = f(r) \left[\frac{f'(r)}{r} + \frac{l(l+1)}{r^2} \right]. \quad (9)$$

After obtaining the effective potential of the black hole, we compare it with the standard Poschl-Teller potential at their maxima. The Poschl-Teller potential has the form [18]:

$$V_{PT} = \frac{V_0}{\cosh^2 a(x - x_0)}, \quad (10)$$

where the quantity V_0 denotes the height and a denotes the curvature of the potential at its maximum. On comparing the two potentials, we get the analytical form of the parameters V_0 and a . Then we utilize the formulae for calculating the QNMs, which is given by Mashhoon as [18]

$$\omega = \omega_0 + i\Gamma = \pm \left(V_0 - \frac{a^2}{4} \right)^{\frac{1}{2}} + ia \left(n + \frac{1}{2} \right). \quad (11)$$

Now, using this formula we have calculated the QNMs of the GUP-corrected black hole surrounded by a quintessential dark energy field as shown in the Table I. In this calculation of QNMs, we have considered a small positive value of the quintessence parameter $e = 0.05$ laying well within the accepted range and mass of the black hole is considered as $M = 1$. The quantum deformation parameters α and β are also assumed as small positive values within their well accepted range as shown in the table.

It is interesting to note that there is a striking dependence of the QNMs on the deformation parameters. As is seen from Table I, when α is kept constant and β is increased, there is a noticeable decrease in the magnitude of the real part of the QNMs. That is, the amplitude of QNMs is inversely proportional to β . Whereas, with a particular value of β , it is seen that the amplitude increases with increase in α . On the other hand in the case of the imaginary part of the QNM representing the damping of the wave, for a fixed value of α , the damping increases with increase in β . While, for a fixed β , the damping decreases with an increase in α . We have also calculated the QNMs for the black hole with $l = 2$ as shown in Table II. Similar pattern is observed in this case also. But one notable feature that comes out is that with an increase in l , the corresponding amplitudes of the QNMs increase noticeably, while the damping factor is not much affected although it decreases with increasing l . Another feature that is apparent from all the calculated modes is that with the increase in n values the amplitude of QNMs remains the same but its damping increases. This is in fact already clear from equation (11).

It will also be interesting to observe any dependence of the QNMs with the quintessence parameter e , which has been kept at a constant value in the previous analysis. For this purpose, as shown in the Table III, we have computed the QNMs for different values of the parameter e with some fixed values of the deformation parameters α and β . It is seen from the table that for a fixed value of l , with increasing e , the amplitude decreases, while the damping increases.

Figs. 2 – 4 give the visual representation of all these behaviours of QNMs of the black hole as discussed and presented in Tables I – III. Fig. 2 shows the variation of the amplitude and damping part of the QNMs with respect to the GUP parameter α for a fixed value of the parameter $\beta = 0.05$ and for three different l values. It is seen that amplitude of QNMs increases slowly, whereas the damping decreases rapidly with the increasing values of α . In Fig. 3 the variations of amplitude and damping of QNMs with respect to β for a fixed value of $\alpha = 0.05$ and for three different l values are shown. This figure shows that the effect of β is totally opposite to that of α on the QNMs. However, the trend of the effect of these two parameters on QNMs is almost

TABLE I: QNMs of the GUP-corrected black hole surrounded by a quintessence field for $n = 0, n = 1, n = 2$ modes, for multipole number $l = 1$, quintessence parameter $e = 0.05$ and various values of the deformation parameter α and β obtained by using the Mashhoon method.

α	β	e	QNMs for $n = 0$	QNMs for $n = 1$	QNMs for $n = 2$	QNMs for $n = 3$
0.00	0.00	0.05	0.269699 + 0.106170i	0.269699 + 0.318511i	0.269699 + 0.530852i	0.269699 + 0.743192i
0.00	0.01	0.05	0.257500 + 0.109324i	0.257500 + 0.327971i	0.257500 + 0.546619i	0.257500 + 0.765267i
0.00	0.02	0.05	0.246116 + 0.111819i	0.246116 + 0.335457i	0.246116 + 0.559095i	0.246116 + 0.782733i
0.00	0.03	0.05	0.235482 + 0.113762i	0.235482 + 0.341287i	0.235482 + 0.568812i	0.235482 + 0.796337i
0.02	0.00	0.05	0.283504 + 0.101997i	0.283504 + 0.305990i	0.283504 + 0.509984i	0.283504 + 0.713977i
0.02	0.01	0.05	0.270366 + 0.105984i	0.270366 + 0.317951i	0.270366 + 0.529919i	0.270366 + 0.741886i
0.02	0.02	0.05	0.258121 + 0.109175i	0.258121 + 0.327526i	0.258121 + 0.545876i	0.258121 + 0.764227i
0.02	0.03	0.05	0.246696 + 0.111702i	0.246696 + 0.335107i	0.246696 + 0.558512i	0.246696 + 0.781916i
0.04	0.00	0.05	0.298387 + 0.096763i	0.298387 + 0.290290i	0.298387 + 0.483817i	0.298387 + 0.677343i
0.04	0.01	0.05	0.284222 + 0.101762i	0.284222 + 0.305286i	0.284222 + 0.508810i	0.284222 + 0.712334i
0.04	0.02	0.05	0.271034 + 0.105795i	0.271034 + 0.317385i	0.271034 + 0.528975i	0.271034 + 0.740565i
0.04	0.03	0.05	0.258744 + 0.109025i	0.258744 + 0.327075i	0.258744 + 0.545124i	0.258744 + 0.763174i
0.06	0.00	0.05	0.314447 + 0.090238i	0.314447 + 0.270713i	0.314447 + 0.451188i	0.314447 + 0.631663i
0.06	0.01	0.05	0.299161 + 0.096470i	0.299161 + 0.289410i	0.299161 + 0.482350i	0.299161 + 0.675289i
0.06	0.02	0.05	0.284942 + 0.101525i	0.284942 + 0.304574i	0.284942 + 0.507623i	0.284260 + 0.712247i
0.06	0.03	0.05	0.271705 + 0.105604i	0.271705 + 0.316812i	0.271705 + 0.528020i	0.271705 + 0.739228i

TABLE II: QNMs of GUP-corrected black hole surrounded by a quintessence field for $n = 0, n = 1, n = 2$ and $n = 3$ modes, for multipole number $l = 2$, quintessence parameter $e = 0.05$ and various values of the deformation parameter α and β obtained by using the Mashhoon method.

α	β	e	QNMs for $n = 0$	QNMs for $n = 1$	QNMs for $n = 2$	QNMs for $n = 3$
0.00	0.00	0.05	0.447498 + 0.102677i	0.447498 + 0.308031i	0.447498 + 0.513384i	0.447498 + 0.718738i
0.00	0.01	0.05	0.430431 + 0.105325i	0.430431 + 0.315974i	0.428658 + 0.527870i	0.430431 + 0.737273i
0.00	0.02	0.05	0.414525 + 0.107389i	0.414525 + 0.322167i	0.414525 + 0.536946i	0.414525 + 0.751724i
0.00	0.03	0.05	0.399674 + 0.108966i	0.399674 + 0.326897i	0.399674 + 0.544828i	0.399674 + 0.762759i
0.02	0.00	0.05	0.466854 + 0.099131i	0.466854 + 0.297394i	0.466854 + 0.495657i	0.466854 + 0.693919i
0.02	0.01	0.05	0.448431 + 0.102519i	0.448431 + 0.307558i	0.448431 + 0.512596i	0.448431 + 0.717635i
0.02	0.02	0.05	0.431299 + 0.105201i	0.431299 + 0.315602i	0.431299 + 0.526004i	0.431299 + 0.736406i
0.02	0.03	0.05	0.415335 + 0.107293i	0.415335 + 0.321880i	0.415335 + 0.536467i	0.415335 + 0.751054i
0.04	0.00	0.05	0.487794 + 0.094643i	0.487794 + 0.283930i	0.487794 + 0.473216i	0.487794 + 0.662503i
0.04	0.01	0.05	0.467862 + 0.098931i	0.467862 + 0.296793i	0.467862 + 0.494654i	0.467862 + 0.692516i
0.04	0.02	0.05	0.449367 + 0.102360i	0.449367 + 0.307079i	0.449367 + 0.511798i	0.449367 + 0.716518i
0.04	0.03	0.05	0.432170 + 0.105075i	0.432170 + 0.315226i	0.432170 + 0.525376i	0.432170 + 0.735527i
0.06	0.00	0.05	0.510501 + 0.089004i	0.510501 + 0.267012i	0.510501 + 0.445020i	0.510501 + 0.623028i
0.06	0.01	0.05	0.488885 + 0.094391i	0.488885 + 0.283172i	0.488885 + 0.471953i	0.488885 + 0.660734i
0.06	0.02	0.05	0.468874 + 0.098728i	0.468874 + 0.296184i	0.468874 + 0.493640i	0.468874 + 0.691096i
0.06	0.03	0.05	0.450307 + 0.102198i	0.450307 + 0.306594i	0.450307 + 0.510991i	0.450307 + 0.715387i

similar. The first two plots of Fig. 4 show the behaviours of amplitude and damping respectively of QNMs of the black hole with respect to quintessence field parameter e for a constant value of $\alpha = \beta = 0.05$ and for two values l . Similar to the case of the parameter β in this case also the amplitude decreases slowly, but the damping increases at a relatively faster step. The third plot of this figure shows the fact that for a fixed l , the damping almost remains constant with increasing quintessence parameter e and the higher values of n give a much higher damping.

TABLE III: QNMs of GUP-corrected black hole surrounded by a quintessence field for $n = 0$, $n = 1$, $n = 2$ and $n = 3$ modes, for multipole number $l = 1$ and $l = 2$, the deformation parameter $\alpha = 0.02$ and $\beta = 0.02$ and various values of the quintessence parameter e obtained by using the Mashhoon method.

l	e	QNMs for $n = 0$	QNMs for $n = 1$	QNMs for $n = 2$	QNMs for $n = 3$
1	0.01	0.278884 + 0.106046i	0.278884 + 0.318139i	0.278884 + 0.530231i	0.278884 + 0.742323i
1	0.03	0.268485 + 0.107679i	0.268485 + 0.323037i	0.268485 + 0.538395i	0.268485 + 0.753753i
1	0.05	0.258121 + 0.109175i	0.258121 + 0.327526i	0.258121 + 0.545876i	0.258121 + 0.764227i
1	0.07	0.247793 + 0.110532i	0.247793 + 0.331597i	0.247793 + 0.552662i	0.247793 + 0.773727i
2	0.01	0.459854 + 0.102496i	0.459854 + 0.307487i	0.459854 + 0.512479i	0.459854 + 0.717470i
2	0.03	0.445542 + 0.103907i	0.445542 + 0.311721i	0.445542 + 0.519535i	0.445542 + 0.727349i
2	0.05	0.431299 + 0.105201i	0.431299 + 0.315602i	0.431299 + 0.526004i	0.431299 + 0.736406i
2	0.07	0.417129 + 0.106375i	0.417129 + 0.319124i	0.417129 + 0.531873i	0.417129 + 0.744623i

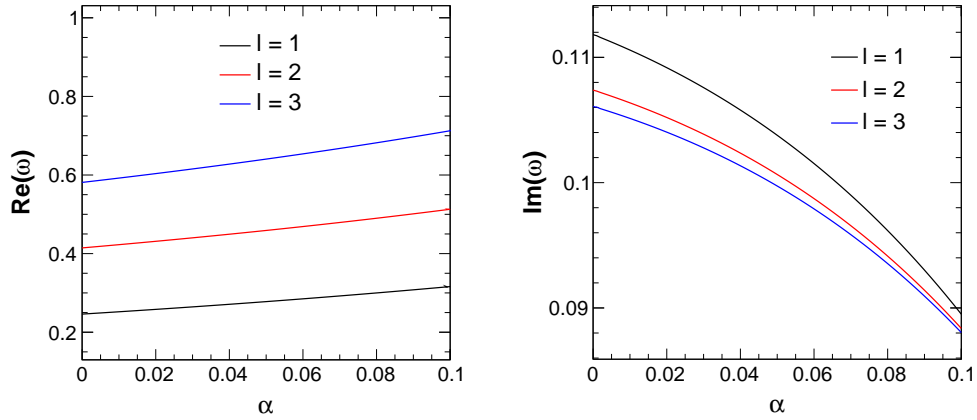


FIG. 2: Behaviours of QNMs with respect to the GUP parameter α for three different values of l with $n = 0$ and $\beta = 0.05$. The amplitude of QNMs increases with an increase in α , while the damping decreases with increasing α (Mashhoon Method).

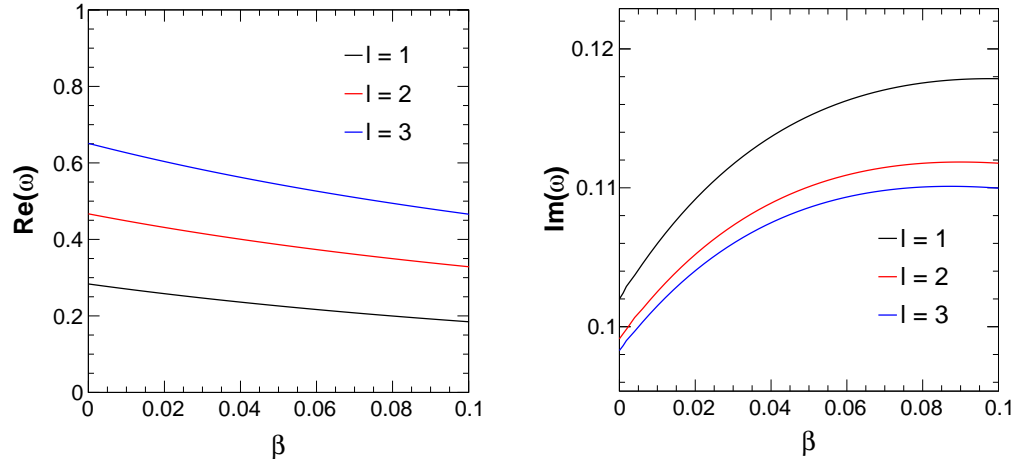


FIG. 3: Behaviours of QNMs with respect to the GUP parameter β for three different values of l with $n = 0$ and $\alpha = 0.05$. The amplitude decreases with an increase in β , while the damping increases with increasing β (Mashhoon Method).

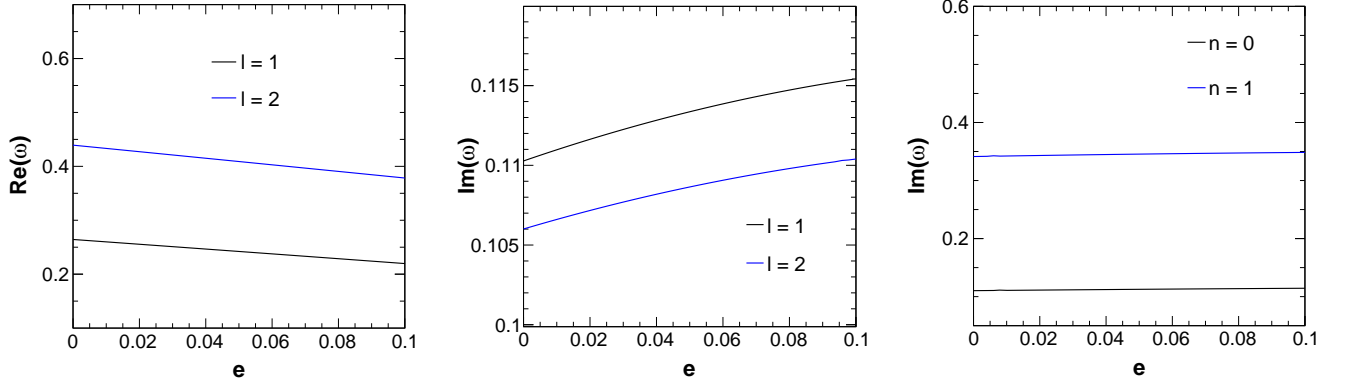


FIG. 4: Behaviours of QNMs with respect to the quintessence parameter e for two different values of l (first two plots with $n = 0$) and two different values n (right plot with $l = 1$) with $\alpha = \beta = 0.05$. The amplitude decreases with an increase in e , while the damping increases with increasing e (Mashhoon Method).

B. QNMs by WKB method

The QNMs can be reliably calculated using the WKB method. It is a semi-analytical approximation method. The basics of the WKB method can be found extensively in literature ([2, 3, 16] and references therein). Here our basic intention is to make a comparative analysis of the QNM frequencies obtained by the Mashhoon method with that will be given by the WKB method.

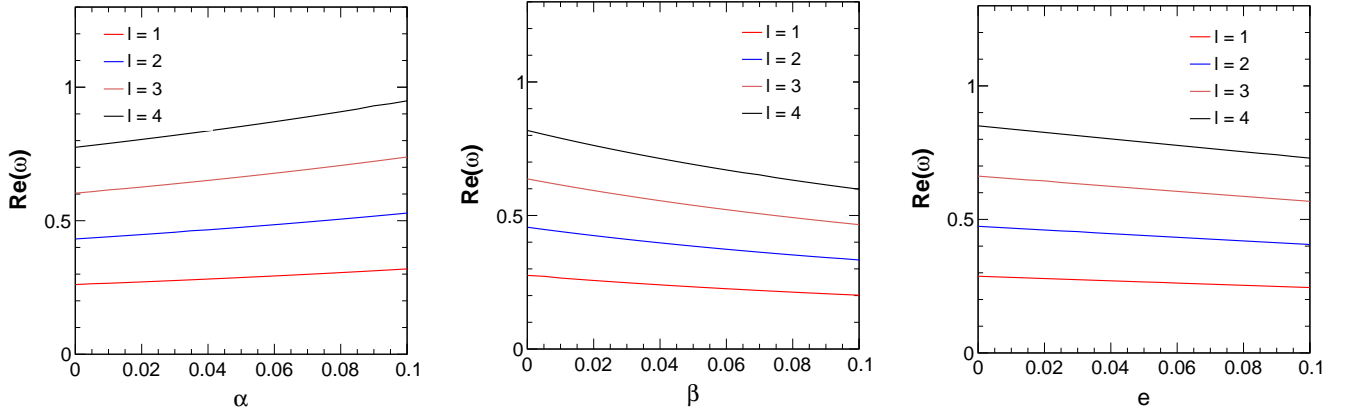


FIG. 5: Variation of amplitude of QNMs with various parameters of the model obtained by using the WKB approximation. The left plot is for $\beta = 0.01$ and $e = 0.05$, the middle plot is for $\alpha = 0.01$ and $e = 0.05$, and the right plot is for $\alpha = \beta = 0.01$.

The perturbation equation of a black hole with a probe that couple minimally to a scalar field, can be conveniently transformed into a Schrödinger-like wave equation given by

$$\frac{d^2\psi}{dx^2} + (\omega^2 - V_l(x))\psi = 0. \quad (12)$$

Here, the tortoise coordinate x is defined as $dx = dr/f(r)$, ω gives the QNM frequencies of the black hole and the effective potential $V_l(x)$ is same as the potential (9) if we replace the coordinate $x \rightarrow r$. For consistency, equation (12) should satisfy some boundary conditions at the horizon and at infinity. Asymptotically flat spacetimes lead to the following quasinormal criteria:

$$\psi(x) \rightarrow \begin{cases} P e^{+i\omega x} & \text{if } x \rightarrow -\infty \\ Q e^{-i\omega x} & \text{if } x \rightarrow +\infty, \end{cases} \quad (13)$$

where P and Q denote constants of integration. Using these conditions we have calculated the QNM frequencies for our considered black hole. The results, i.e. the amplitude and damping of QNMs or the real and imaginary parts of QNM frequencies

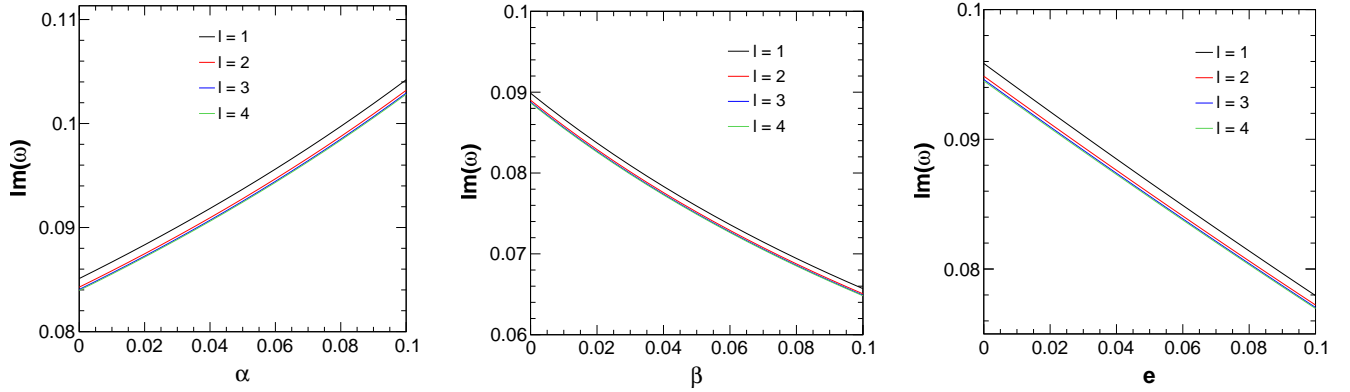


FIG. 6: Variation of damping of QNMs with various parameters of the model obtained by using the WKB approximation. The left plot is for $\beta = 0.01$ and $e = 0.05$, the middle plot is for $\alpha = 0.01$ and $e = 0.05$, and the right plot is for $\alpha = \beta = 0.01$.

have been plotted against the GUP and the quintessence parameters as shown in Figs. 5 and 6. Fig. 5 shows the trends of variations of the real parts of the QNMs with respect to variations in α , β and e . It is clear that these trends are the same with the amplitude obtained by the Mashhoon method, but in this case the value of the amplitude is slightly greater than that obtained by the Mashhoon method. Whereas the damping of the QNMs shows the opposite behaviour with the Mashhoon method. However, it is to be noted that in WKB method, the variation of damping term is insignificant with respect to variation in all the model parameters.

Tables IV and V show a clear comparison between the Mashhoon method and the WKB method. Table IV is for the $n = 0$ case and Table V is for the $n = 1$. For $n = 0$ we found that the real part of the QNM calculated by the two methods agree to a good extent while the imaginary part of the modes vary to some extent. There is a far better agreement between two methods for higher l values. From Table IV one can observe the following additional points. For the given values of l , β and e with increase in α values, there is an increasing mismatch between the two methods. On the other hand, for the given values of l , α and e with increasing values of β there is a better match between the methods. Moreover, for the given values of l , α and β , increasing e values lead to decrease in mismatch between the methods. However, from Table V it is seen that some of the above observations are not applicable to the case for $n = 1$ and the difference between the Mashhoon method and the WKB method in this case is almost ten times higher than that for the $n = 0$ case. This may be due to the fact that the usual WKB method can only be reliably used to calculate QNMs for the situation with $n < l$ [2, 16].

III. THERMODYNAMIC PROPERTIES OF THE BLACK HOLE

The notion of a minimal length scale does not exist in the normal Heisenberg algebra, but in the Planck energy scales, taking into consideration the effects of gravity, it becomes necessary. The introduction of the GUP is thus naturally motivated and leads to interesting results. The temperature of the Schwarzschild black hole is usually expressed in the form [86]:

$$T = \frac{\kappa}{8\pi} \frac{dA}{dS}, \quad (14)$$

where κ is the surface gravity of the black hole, A is the surface area and S is the entropy of the black hole. Calculations yield the expression for the surface gravity at the horizon in our case as

$$\kappa = - \lim_{r \rightarrow r_H} \sqrt{-\frac{g^{11}}{g^{00}}} \frac{(g^{00})'}{g^{00}} = \frac{1}{r_H} \left(1 + \frac{3e\omega}{r_H^{3\omega+1}} \right), \quad (15)$$

where the GUP corrected horizon radius r_{hGUP} of the black hole is denoted as r_H . Liang [86] showed that the area of a black hole increases proportionately when it absorbs a particle of particular mass and size. A minimal change in area means a minimal change in entropy, which can have the smallest possible value of $\ln 2$ according to the information theory. So, we can express the ratio $\frac{dA}{dS}$ as

$$\frac{dA}{dS} = \frac{(\Delta A)_{min}}{(\Delta S)_{min}} = \frac{\epsilon \Delta x \Delta p}{\ln 2} = \frac{\epsilon(4r_H + \alpha)r_H}{\beta \ln 2} \left[1 - \sqrt{1 - \frac{4\beta}{(4r_H + \alpha)^2}} \right]. \quad (16)$$

TABLE IV: Comparison of QNMs of GUP-corrected black hole surrounded by a quintessence field obtained by using the Mashhoon method and the 6th order WKB method for $n = 0$, $l = 1, 2, 3, 4$, and for various values of the parameters α , β and e . Here $\Delta|\omega_M - \omega_{WKB}|$ represents the absolute difference between the QNM frequencies calculated by using the Mashhoon method and the WKB method.

Multipole	α	β	e	Mashhoon Method	WKB method	$\Delta \omega_M - \omega_{WKB} $
$l = 1$	0.01	0.01	0.03	0.274715 + 0.105993i	0.274250 + 0.090298i	5.7204×10^{-3}
	0.01	0.01	0.05	0.263814 + 0.107754i	0.265742 + 0.086685i	5.4485×10^{-3}
	0.01	0.03	0.05	0.240990 + 0.112803i	0.248128 + 0.080939i	5.0885×10^{-3}
	0.05	0.01	0.05	0.291550 + 0.099263i	0.287202 + 0.093685i	5.8888×10^{-3}
$l = 2$	0.01	0.01	0.03	0.454274 + 0.102489i	0.453426 + 0.089402i	3.5361×10^{-3}
	0.01	0.01	0.05	0.439261 + 0.104011i	0.439746 + 0.085840i	3.3614×10^{-3}
	0.01	0.03	0.05	0.407365 + 0.108192i	0.410599 + 0.080150i	3.1389×10^{-3}
	0.05	0.01	0.05	0.478163 + 0.096792i	0.475258 + 0.092772i	3.6331×10^{-3}
$l = 3$	0.01	0.01	0.03	0.634124 + 0.101454i	0.633405 + 0.089164i	2.5386×10^{-3}
	0.01	0.01	0.05	0.614233 + 0.102908i	0.614444 + 0.085616i	2.4137×10^{-3}
	0.01	0.03	0.05	0.571617 + 0.106832i	0.573718 + 0.079941i	2.2538×10^{-3}
	0.05	0.01	0.05	0.666197 + 0.096067i	0.664065 + 0.092530i	2.6074×10^{-3}
$l = 4$	0.01	0.01	0.03	0.814241 + 0.101021i	0.813646 + 0.089066i	1.9775×10^{-3}
	0.01	0.01	0.05	0.789248 + 0.102448i	0.789370 + 0.085524i	1.8798×10^{-3}
	0.01	0.03	0.05	0.735481 + 0.106263i	0.737049 + 0.079855i	1.7553×10^{-3}
	0.05	0.01	0.05	0.854793 + 0.095764i	0.853116 + 0.092430i	2.0321×10^{-3}

TABLE V: Comparison of QNMs of GUP-corrected black hole surrounded by a quintessence field obtained by using the Mashhoon method and the 6th order WKB method for $n = 1$, $l = 1, 2, 3, 4$, and for various values of the parameters α , β and e . Here $\Delta|\omega_M - \omega_{WKB}|$ represents the absolute difference between the QNM frequencies calculated by using the Mashhoon method and the WKB method.

Multipole	α	β	e	Mashhoon Method	WKB method	$\Delta \omega_M - \omega_{WKB} $
$l = 1$	0.01	0.01	0.03	0.274715 + 0.317980i	0.248160 + 0.282859i	4.3926×10^{-2}
	0.01	0.01	0.05	0.263814 + 0.323261i	0.240814 + 0.271373i	5.4432×10^{-2}
	0.01	0.03	0.05	0.240990 + 0.338408i	0.224852 + 0.253387i	7.6679×10^{-2}
	0.05	0.01	0.05	0.291550 + 0.297790i	0.260262 + 0.293288i	2.4635×10^{-2}
$l = 2$	0.01	0.01	0.03	0.454274 + 0.307466i	0.435359 + 0.272995i	3.4672×10^{-2}
	0.01	0.01	0.05	0.439261 + 0.312032i	0.422543 + 0.262032i	4.1613×10^{-2}
	0.01	0.03	0.05	0.407365 + 0.324575i	0.394536 + 0.244664i	5.6619×10^{-2}
	0.05	0.01	0.05	0.478163 + 0.290375i	0.456666 + 0.283193i	2.2079×10^{-2}
$l = 3$	0.01	0.01	0.03	0.634124 + 0.304361i	0.620011 + 0.269992i	2.7137×10^{-2}
	0.01	0.01	0.05	0.614233 + 0.308725i	0.601704 + 0.259200i	3.2296×10^{-2}
	0.01	0.03	0.05	0.571617 + 0.320496i	0.561822 + 0.242020i	4.3601×10^{-2}
	0.05	0.01	0.05	0.666197 + 0.288200i	0.650296 + 0.280132i	1.7796×10^{-2}
$l = 4$	0.01	0.01	0.03	0.814241 + 0.303063i	0.803072 + 0.268725i	2.1973×10^{-2}
	0.01	0.01	0.05	0.789248 + 0.307343i	0.779316 + 0.258007i	2.6063×10^{-2}
	0.01	0.03	0.05	0.735481 + 0.318789i	0.727662 + 0.240906i	3.5094×10^{-2}
	0.05	0.01	0.05	0.854793 + 0.287293i	0.842251 + 0.278843i	1.4571×10^{-2}

Here, the uncertainties in momentum and position are connected with the mass and size of the particle falling into the black hole respectively and ϵ is the calibration factor [66]. Using equations (15) and (16) into (14), we have the following expression for the GUP-corrected temperature,

$$T_{GUP} = \frac{1}{8\pi} \left(1 + \frac{3e\omega}{r_H^{3\omega+1}} \right) \frac{\epsilon(4r_H + \alpha)}{\beta \ln 2} \left[1 - \sqrt{1 - \frac{4\beta}{(4r_H + \alpha)^2}} \right]. \quad (17)$$

The above expression of temperature modifies into a simpler form in absence of the quintessence and the deformation parameters, which must be equal to the Hawking temperature $\frac{1}{4\pi r_H}$. Thus, the factor ϵ is determined to be $4 \ln 2$ and we have the final form

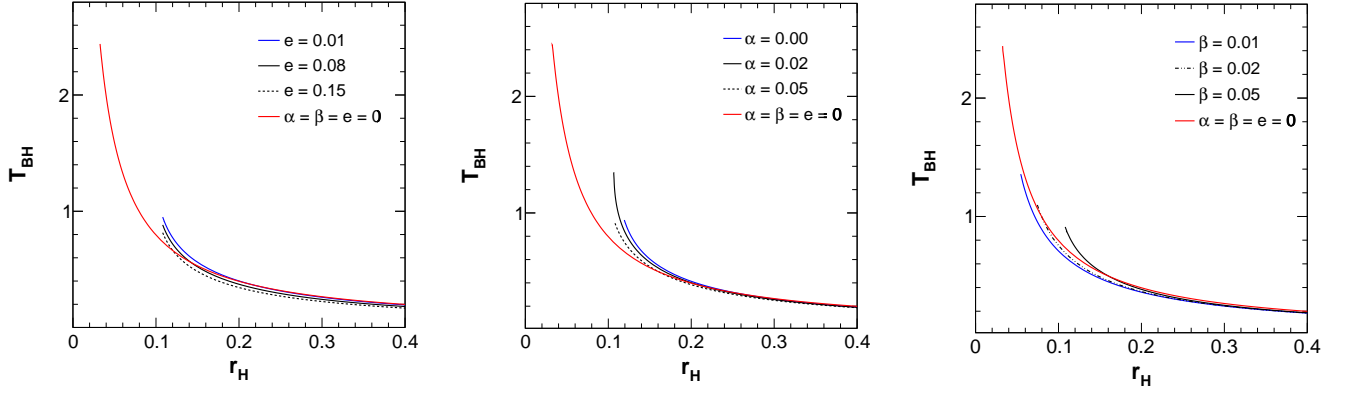


FIG. 7: Variation of the GUP-corrected black hole temperature with quintessence parameter e for $\alpha = \beta = 0.05$ (left plot), with α considering $\beta = e = 0.05$ (middle plot) and with β keeping $\alpha = e = 0.05$ (right plot). In all three plots the solid red line represents the Schwarzschild black hole temperature.

of the GUP-modified black hole temperature as

$$T_{GUP} = \frac{(4r_H + \alpha)}{2\pi\beta} \left(1 + \frac{3e\omega}{r_H^{3\omega+1}}\right) \left[1 - \sqrt{1 - \frac{4\beta}{(4r_H + \alpha)^2}}\right]. \quad (18)$$

For $\omega = -\frac{1}{3}$, the expression for the GUP-corrected temperature can be simplified as

$$T_{GUP} = \frac{(4r_H + \alpha)}{2\pi\beta} (1 - e) \left[1 - \sqrt{1 - \frac{4\beta}{(4r_H + \alpha)^2}}\right]. \quad (19)$$

It is interesting to note that the introduction of GUP corrections lead to the dependency of the temperature on the deformation parameters α and β , apart from the quintessence parameter e . In absence of the deformation parameters, the HUP-corrected temperature of the Schwarzschild black hole surrounded by quintessence is given by

$$T_{HUP} = \frac{1}{4\pi r_H} \left(1 + \frac{3e\omega}{r_H^{3\omega+1}}\right). \quad (20)$$

Considering real-valued temperature, it can be seen from the above equation (19) that for $\omega = -\frac{1}{3}$, there exists some bounds on the horizon of the black hole depending on the values of α and β [66], since the term inside the square root can not be negative. This is illustrated by the plots of temperature vs horizon graphs shown in Fig. 7, which clearly shows the dependence as mentioned. From this figure it is clear that introduction of quantum corrections due to the generalized uncertainty principle and the surrounding quintessence field have some influence on the black hole temperature. In some cases the influence looks significant for black holes with small event horizon radii. Whereas for black holes with large event horizon radius influence looks insignificant. In all the cases, temperature seems to decrease with the increase in horizon radius. Thus, black holes with very large event horizon radii might have sub-zero temperatures associated with them. The temperature profiles obtained here are in good agreement with results presented in [66, 87].

Another interesting aspect of black hole physics is the study of the remnant formation, which is considered to be a stable state of the black hole that does not emit any heat and whose mass is reduced due to the evaporation. In this context the dependency of heat capacity of the black hole on the GUP parameters becomes an important feature that we want to analyze. For this purpose, we make use of the thermodynamic relation connecting the heat capacity C of the black hole, its mass M and temperature T as given below:

$$C = \frac{dM}{dT}.$$

From this relation, we derive the expression for the GUP-corrected heat capacity of the black hole as

$$C_{GUP} = - \frac{\pi\beta \left(4\alpha(1-e) + r_H \left(\sqrt{\frac{(e-1)^2((4\alpha+r_H)^2-64\beta)}{r_H^2}} - e + 1\right)\right) ((\alpha + 4r_H)^2 - 4\beta)}{8r_H \sqrt{\frac{(e-1)^2((4\alpha+r_H)^2-64\beta)}{r_H^2}} ((g-1)(\alpha + 4r_H)^2 + 4\beta)}, \quad (21)$$

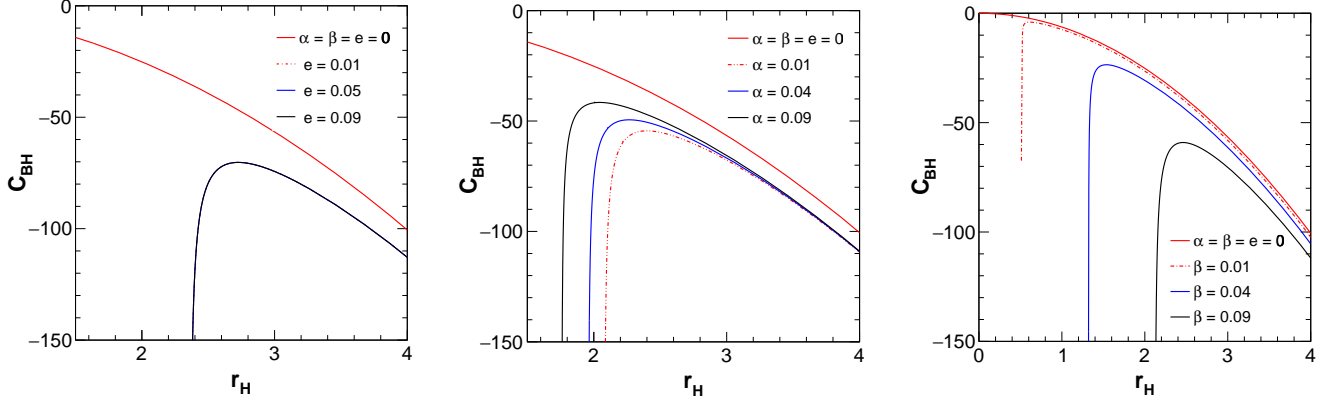


FIG. 8: Variation of the GUP-corrected heat capacity of the black hole C_{BH} in terms of horizon radius r_H for varying e values with $\alpha = 0.01$ and $\beta = 0.09$ (left plot), for varying α values with $\beta = e = 0.07$ (middle plot) and for varying values of β with $\alpha = 0.07$ and $e = 0.05$ (right plot). In all three plots the solid red line represents the heat capacity of Schwarzschild black hole.

where we have introduced a term g defined as $g = \sqrt{1 - \frac{4\beta}{(4r_H + \alpha)^2}}$ and considered $\omega = -\frac{1}{3}$. Fig. 8 shows the variation of heat capacity function (21) with the horizon radius for different values of e , α and β considering $\omega = -\frac{1}{3}$ and $M = 1$. It is seen that the heat capacity is independent of the quintessence field, but depends heavily on the GUP-parameters α and β . This dependence is more pronounced on the parameter β , especially for small horizon radii black holes. In almost all the cases the heat capacity is significantly different from the case of the Schwarzschild black hole. The heat capacity is negative throughout, which is very large for the small horizon radii black holes as well as for the cases of large radii ones. Thus GUP-corrected black holes lose more energy in the form of radiation than that of the Schwarzschild black hole, in particular, by small and large horizon radii black holes.

As already stated, when a black hole is not exchanging any heat with its surrounding, then we call this stable state as the remnant of the black hole. In this case, the heat capacity becomes zero. From the above expression, it can be shown that for the existence of remnant, the expression of the horizon radius of the remnant comes out as

$$r_{rem} = \frac{1}{4} (2\sqrt{\beta} - \alpha). \quad (22)$$

Thus, the remnant horizon radius depends on the deformation parameters α and β , and is independent of the behaviour of the surrounding field. It is interesting to note that in Ref. [66], this dependency was established with one parameter only. The expression for the remnant temperature is calculated as

$$T_{rem} = \frac{3e\omega \left(\frac{\sqrt{\beta}}{2} - \frac{\alpha}{4} \right)^{-(3\omega+1)} + 1}{\pi\sqrt{\beta}}. \quad (23)$$

For instance, the remnant temperature for a particular combination of $\alpha = 0.05$, $\beta = 0.05$, $e = 0.05$ and $\omega = -\frac{1}{3}$ comes out to be 1.352, which is above the upper limit of $T_{GUP} \leq 1.210$ for this case as obtained from the equation (18). This upper limit of T_{GUP} is calculated from the condition that

$$\sqrt{1 - \frac{4\beta}{(4r_H + \alpha)^2}} \geq 0,$$

which gives minimum allowed horizon radius for this case as ~ 0.1 . This implies that the GUP-corrected Schwarzschild black holes in our study can not reach the stage of the remnant, which is also clear from the heat capacity analysis above.

The entropy function of the black hole can be estimated from the thermodynamic relation,

$$S = \int \frac{dM}{T} \quad (24)$$

which, with the help of equations (8) and (18), can be expressed for the GUP-corrected black hole as

$$S_{GUP} = \frac{\pi M^2 ((a+1)(\alpha + 4r_H)^2 - 4\beta \log((a+1)(\alpha + 4r_H)))}{32(M^2 - 4\beta(e-1)^2)}. \quad (25)$$

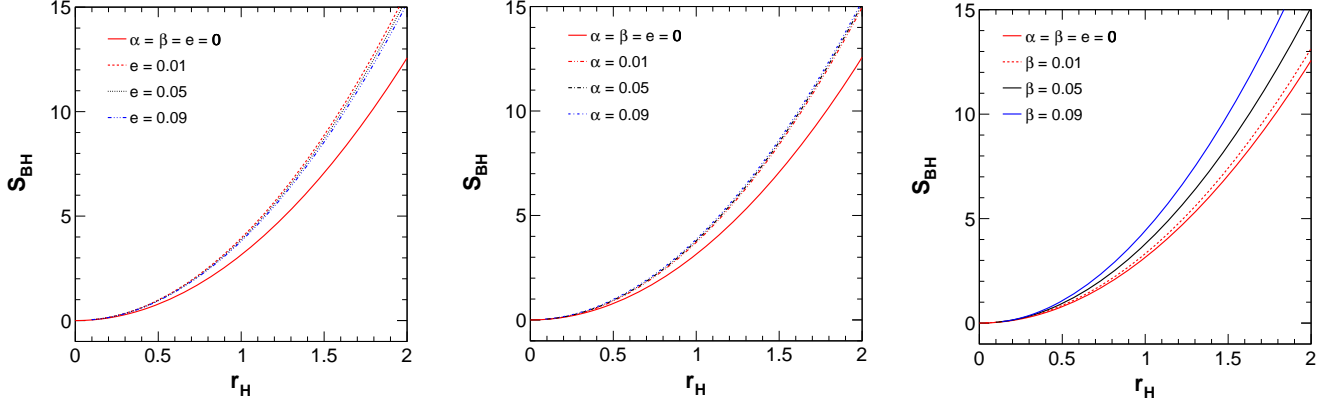


FIG. 9: Variation of entropy of GUP-corrected black holes with respect to horizon radius for different values of e with $\alpha = \beta = 0.05$ (left plot), for different values of α with $e = 0.1$ and $\beta = 0.05$ (middle plot), and for different values of β with $e = 0.1$ and $\alpha = 0.05$ (right plot). In all three plots the solid red line represents the entropy of Schwarzschild black holes.

Fig. 9 shows the variations of the entropy function (25) with respect to the horizon radius of the GUP-corrected black holes for different values of the model's parameters together with the same for the Schwarzschild black holes. It is observed that the parameter e and α have a very negligible impact on the entropy of the black holes. Whereas, the parameter β has a significant impact on the entropy of black holes with sufficient horizon radii [66]. Moreover, the entropy of the GUP-corrected black holes is found to be higher than that of the Schwarzschild black holes for almost all cases and for sufficient horizon radius. This difference is substantial for a black hole with a larger horizon radius depending on the value of model parameter β .

Black hole shadow is a dark area surrounding the black hole and caused by its gravitational lensing and light ray capturing. Generally, for a static and spherically symmetric case, the shadow is circular, but when rotating black holes are considered, there is an elongation in the direction of rotation. In our case, the black holes are chosen to be spherically symmetric and hence the condition for finding the radius of photon sphere of our black holes is [76]

$$2 - \frac{r f'(r)}{f(r)} = 0. \quad (26)$$

The solution of the above equation gives us the radius of the photon sphere as

$$r_{ps} = \frac{12\beta(1-e)}{M} + \frac{3M}{1-e} - 6\alpha. \quad (27)$$

The shadow radius can be found out from the following expression [76]:

$$R_s = \frac{r_{ps}}{\sqrt{f(r)_{r \rightarrow r_{ps}}}}. \quad (28)$$

The final expression for the shadow radius of our black holes as a function of α , β , e and M can be found as

$$R_s = \frac{3\sqrt{3} \left(4\beta(1-e)^2 - 2\alpha(1-e)M + M^2 \right)}{(1-e)^{3/2} M}. \quad (29)$$

We have plotted the shadow radius versus the deformation parameters α and β , and the quintessential parameter e in Fig. 10. All the plots show a linear relationship between the radius and the parameters. That is the shadow radius decreases linearly with α , whereas it increases linearly with β and e . Moreover, Fig. 11 shows the shadow radius variations in celestial coordinates X and Y [74, 76]. This figure also shows a similar trend of shadows of GUP-corrected black holes with respect to parameters α , β and e as stated above.

IV. CONCLUSION

The primary objective of this work is to study the effects of the deformation parameters introduced by the GUP on the QNMs of oscillation of the Schwarzschild black holes, together with a brief review of the thermodynamic properties of such GUP-corrected

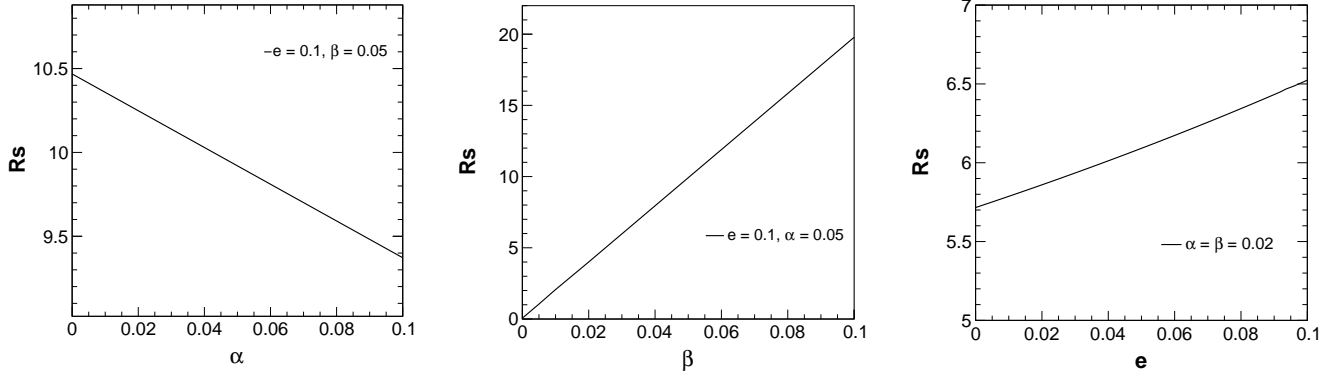


FIG. 10: Shadow radius of GUP-corrected black holes versus model parameter curves for different values of the non-varying parameters at each specific case.

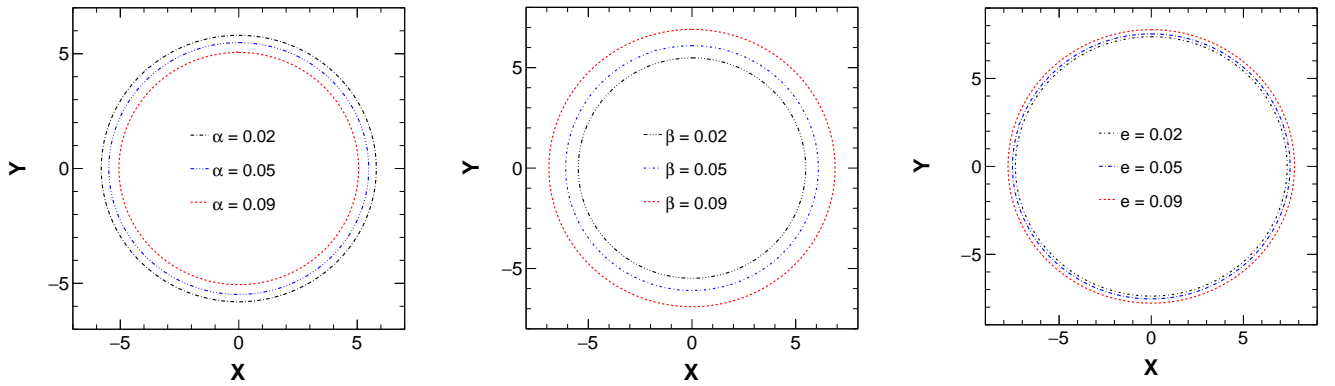


FIG. 11: Variation of shadow radius in celestial coordinate plane [74, 76] with parameters α , β and e . Here, $\beta = 0.02$ and $e = 0.05$ for the first plot, $\alpha = 0.05$ and $e = 0.05$ for the second plot and $\alpha = 0.02$ and $\beta = 0.02$ for the third plot.

black holes surrounded by a quintessence dark energy field. It has been observed that both the deformation parameters as well as the quintessence parameter play an important role on the behaviour of the QNMs of the black holes. We employed two methods for obtaining the QNMs, namely the Mashhoon method and the WKB method. Further we derive a GUP-modified temperature expression of the black holes and show its dependence on the deformation parameters as well as on the quintessence parameter. It is seen that there exist an upper bound on the temperature, which is impacted by the deformation parameters. Further, the heat capacity along with entropy have been evaluated for the GUP-corrected black holes and existence of black hole remnants has been studied. The existence of remnant radius and remnant temperature are certainly impacted by the deformation parameters. We observed that the GUP-corrected black holes can not reach the state of remnant. It is also seen that the quintessence field and the first deformation parameter have no effective roles in the entropy of the black holes, which is dependent only on the second deformation parameter. The shadow radius of the GUP-corrected black hole has been calculated and its dependence on various parameters has been shown. It is quite remarkable that the introduction of small quantum corrections to the black hole metric can have notable influence on various properties of the black holes. This avenue has been investigated in the literature for many years but there are further scopes in this direction apart from the present study. It will be interesting to analyze the impact of these deformations on black hole properties, considering various Modified Theories of Gravity (MTGs).

It is to be noted that once perturbed, a black hole responds by radiating GWs, which evolve in time. This evolution process is divided into three phases, an instant outburst of radiation, a longer period of damped oscillations (QNMs) and at very late times, a suppressed power-law tail [2]. Since we have been able to detect the first phase of GW only, it remains a challenge for the physicists and engineers to develop and improve the sensitivity of modern day detectors so that the second phase of GW can be detected. Steps in this direction have already been undertaken in the means of ambitious future projects like the LISA [88] and the Einstein Telescope [89], which is believed to have far better sensitivity than the present detectors. The prospect of detection of QNMs by LISA has been analysed in Ref. [83]. The detection of QNMs of the black hole can have many useful implications. It can be used to constrain the GUP parameters and as testing grounds for various MTGs as well. These upcoming advanced detectors of GWs can shed more light into this field and provide data for validating various models available at present times,

which is one of the primary objectives in this field of study.

-
- [1] For an introductory account, please refer to [official LIGO website](#).
- [2] R. A. Konoplya and A. Zhidenko, *Quasinormal modes of black holes: From astrophysics to string theory*, *Rev. Mod. Phys.* **83**, 793 (2011).
- [3] R. A. Konoplya, *Quasinormal modes of a small Schwarzschild–anti-de Sitter black hole*, *Phys. Rev. D* **66**, 044009 (2002).
- [4] M. Maggiore, *Gravitational wave experiments and early universe cosmology*, *Phys. Reports* **331**, 6 (2000).
- [5] S. A. Hughes, *Gravitational wave astronomy and cosmology*, *Physics of the Dark Universe* **4**, 86 (2014).
- [6] B. P. Abbott et al., *Observation of Gravitational Waves from a Binary Black Hole Merger*, *Phys. Rev. Lett.* **116**, 061102 (2016).
- [7] B. P. Abbott et al., *Observation of Gravitational Waves from a 22-Solar-Mass Binary Black Hole Coalescence*, *Phys. Rev. Lett.* **116**, 241103 (2016).
- [8] B. P. Abbott et al., *Observation of Gravitational Waves from a Binary Neutron Star Inspiral*, *Phys. Rev. Lett.* **119**, 161101 (2017).
- [9] B. P. Abbott et al., *Observation of a Binary-Black-Hole Coalescence with Asymmetric Masses*, *Phys. Rev. D* **102**, 043015 (2020).
- [10] R. Abbott et al., *Observation of Gravitational Waves from Two Neutron Star–Black Hole Coalescences*, *ApJL* **915**, L5 (2021).
- [11] H. -J. Blome and B. Mashhoon, *Quasi-normal oscillations of a schwarzschild black hole*, *Phys. Lett. A* **100**, 5 (1984).
- [12] S. Chandrasekhar and S. Detweiler, *The quasi-normal modes of the Schwarzschild black hole*, *Proc. Roy. Soc A* **344**, 1639 (1975).
- [13] R. A. Konoplya, *Quasinormal Modes of the Electrically Charged Dilaton Black Hole*, *General Relativity and Gravitation* **34**, 329 (2002).
- [14] R. A. Konoplya, *Quasinormal behavior of the D-dimensional Schwarzschild black hole and the higher order WKB approach*, *Phys. Rev. D* **68**, 024018 (2003).
- [15] D. J. Gogoi and U. D. Goswami, *Gravitational Waves in f(R) Gravity Power Law Model*, *Indian J. Phys.* **96**, 637 (2022).
- [16] D. J. Gogoi and U. D. Goswami, *Quasinormal Modes of Black Holes with Non-Linear-Electrodynamic Sources in Rastall Gravity*, *Physics of the Dark Universe* **33**, 100860 (2021).
- [17] D. J. Gogoi, R. Karmakar and U. D. Goswami, *Quasinormal Modes of Non-Linearly Charged Black Holes surrounded by a Cloud of Strings in Rastall Gravity*, [arXiv:2111.00854 \[gr-qc\]](#) (2022).
- [18] V. Ferrari and B. Mashhoon, *New approach to quasinormal modes of a black hole*, *Phys. Rev. D* **30**, 295 (1984).
- [19] V. Ferrari and B. Mashhoon, *Oscillations of a Black Hole*, *Phys. Rev. Lett.* **52**, 1361 (1984).
- [20] B. Mashhoon et al., *On the gravitational effects of rotating masses: The Thirring-Lense papers*, *General Relativity and Gravitation* **16**, 711 (1984).
- [21] S. Iyer and C. M. Will, *Black-hole normal modes: A WKB approach. I. Foundations and application of a higher-order WKB analysis of potential-barrier scattering*, *Phys. Rev. D* **35**, 3621 (1987).
- [22] B. F. Schutz and C. M. Will, *Black hole normal modes - A semianalytic approach*, *The Astrophysical Journal* **291**, L33 (1985).
- [23] R. A. Konoplya et al., *Higher order WKB formula for quasinormal modes and grey-body factors: recipes for quick and accurate calculations*, *Class. Quantum Grav.* **36**, 155002 (2019).
- [24] E. W. Leaver, *An analytic representation for the quasi-normal modes of Kerr black holes*, *Proc. R. Soc. Lond. A* **402**, 285 (1985).
- [25] E. W. Leaver, *Quasinormal modes of Reissner-Nordström black holes*, *Phys. Rev. D* **41**, 2986 (1990).
- [26] V. Cardoso et al., *Quasinormal modes and stability of the rotating acoustic black hole: Numerical analysis*, *Phys. Rev. D* **70**, 124032 (2004).
- [27] A. Karlos, S. J. Elliott and J. Cheer, *Higher-order WKB analysis of reflection from tapered elastic wedges*, *Journal of Sound and Vibration* **449**, 368 (2019).
- [28] A. Zhidenko, *Quasi-normal modes of the scalar hairy black hole*, *Class. Quantum Grav.* **23**, 3155 (2006).
- [29] A. Zhidenko, *Quasi-normal modes of Schwarzschild–de Sitter black holes*, *Class. Quantum Grav.* **21**, 273 (2003).
- [30] M. Okyay and A. Övgün, *Nonlinear electrodynamic effects on the black hole shadow, deflection angle, quasinormal modes and greybody factors*, *JCAP* **01**, 009 (2022).
- [31] I. Güllü and A. Övgün, *Schwarzschild-like black hole with a topological defect in bumblebee gravity*, *Annals of Physics*, **436**, 168721 (2022).
- [32] H. Nandan et al., *Black Hole Solutions and Pressure Terms in Induced Gravity with Higgs Potential*, *Class. Quant. Grav.* **27**, 245003 (2010).
- [33] S. Kala et al., *Geodesics and Bending of Light around a BTZ Black Hole Surrounded by Quintessential Matter*, *Mod. Phys. Lett. A* **36**, No. 31, 2150224 (2021).
- [34] M. M. Caldarelli, G. Cognola and D. Klemm, *Thermodynamics of Kerr-Newman-AdS black holes and conformal field theories*, *Class. Quantum Grav.* **17**, 399 (2000).
- [35] D. N. Page, *Hawking radiation and black hole thermodynamics*, *New J. Phys.* **7**, 203 (2005).
- [36] T. Jacobson and A. C. Wall, *Black Hole Thermodynamics and Lorentz Symmetry*, *Found. Phys.* **40**, 1076 (2010).
- [37] B. Zhang, *Entropy in the interior of a black hole and thermodynamics*, *Phys. Rev. D* **92**, 081501 (2015).
- [38] M. Appels, R. Gregory and D. Kubiznak, *Thermodynamics of Accelerating Black Holes*, *Phys. Rev. Lett.* **117**, 131303 (2016).
- [39] M. Astorino, *Thermodynamics of regular accelerating black holes*, *Phys. Rev. D* **95**, 064007 (2017).
- [40] M. Dehghani, *Thermodynamics of novel charged dilaton black holes in gravity’s rainbow*, *Phys. Lett. B* **785**, 274 (2018).
- [41] C. H. Bayraktar, *Thermodynamics of regular black holes with cosmic strings*, *Eur. Phys. J. C* **133**, 377 (2018).
- [42] Y. Yao, M. -S. Hou and Y. C. Ong, *A complementary third law for black hole thermodynamics*, *Eur. Phys. J. C* **79**, 513 (2019).
- [43] M. Sharif and H. S. Nawaz, *Thermodynamics of rotating regular black holes*, *Chin. Phys. C* **67**, 193 (2020).

- [44] M. Fathi, M. Molina and J. R. Villanueva, *Adiabatic evolution of Hayward black hole*, *Phys. Lett. B* **820**, 136548 (2021).
- [45] S. W. Hawking, *Particle creation by black holes*, *Commun. Math.* **43**, 199 (1975).
- [46] J. M. Bardeen, B. Carter and S. W. Hawking, *The four laws of black hole mechanics*, *Commun. Math* **31**, 161 (1973).
- [47] S. W. Hawking and D. N. Page, *Thermodynamics of black holes in anti-de Sitter space*, *Commun. Math.* **87**, 577 (1983).
- [48] J. D. Bekenstein, *Black Holes and Entropy*, *Phys. Rev. D* **7**, 2333 (1973).
- [49] J. D. Bekenstein, *Generalized second law of thermodynamics in black-hole physics*, *Phys. Rev. D* **9**, 3292 (1974).
- [50] J. D. Bekenstein, *Black Holes and the Second Law*, *Lettere al Nuovo Cimento* **4**, 737 (1972).
- [51] A. G. Riess et al., *Observational Evidence from Supernovae for an Accelerating Universe and a Cosmological Constant*, *The Astronomical Journal* **116**, 1009 (1998).
- [52] S. Perlmutter et al., *Measurements of Ω and Λ from 42 High-Redshift Supernovae*, *ApJ* **517**, 565 (1999).
- [53] E. J. Copeland, M. Sami, and S. Tsujikawa, *Dynamics of Dark Energy*, *Int. J. Mod. Phys. D* **15**, 1753 (2006).
- [54] L. Amendola and S. Tsujikawa, *Dark Energy: Theory and Observations* (Cambridge University Press, Cambridge, 2010).
- [55] Y. Fujii, *Origin of the gravitational constant and particle masses in scale invariant scalar-tensor theory*, *Phys. Rev. D* **26**, 2580 (1982).
- [56] L. H. Ford, *Cosmological constant damping by unstable scalar fields*, *Phys. Rev. D* **35**, 2339 (1987).
- [57] B. Ratra and P. J. E. Peebles, *Cosmological consequences of a rolling homogeneous scalar field*, *Phys. Rev. D* **37**, 3406 (1988).
- [58] S. M. Carroll, *Quintessence and the rest of the world*, *Phys. Rev. Lett.* **81**, 3067 (1998).
- [59] E. J. Copeland, A. R. Liddle and D. Wands, *Exponential potentials and cosmological scaling solutions*, *Phys. Rev. D* **57**, 4686 (1998).
- [60] V. V. Kiselev, *Quintessence and black holes*, *Class. Quantum Grav.* **20**, 1187 (2003).
- [61] S. Chen, B. Wang and R. Su, *Hawking radiation in a d -dimensional static spherically symmetric black hole surrounded by quintessence*, *Phys. Rev. D* **77**, 124011 (2008).
- [62] W. Yi-Huan and R. Jun, *Thermodynamic properties of Reissner-Norstrom-de Sitter quintessence black holes*, *Chin. Phys. B* **22**, 030402 (2012).
- [63] S. Fernando, *Nariai Black Holes with Quintessence*, *Mod. Phys. Lett. A* **28**, 1350189 (2013).
- [64] Md. Shahjalal, *Thermodynamics of quantum-corrected Schwarzschild black hole surrounded by quintessence*, *Nucl. Phys. B* **940**, 63 (2019).
- [65] M. A. Anacleto, F. A. Brito, J. A. V. Campos, and E. Passos, *Quantum-corrected scattering and absorption of a Schwarzschild black hole with GUP*, *Phys. Lett. B* **810**, 135830 (2020).
- [66] B. C. Lütfüoğlu, B. Hamil and L. Dahbi, *Thermodynamics of Schwarzschild black hole surrounded by quintessence with generalized uncertainty principle*, *EPJP* **136**, 976 (2021).
- [67] R. Ndongmo et al., *Thermodynamics of a rotating and non-linear magnetic-charged black hole in the quintessence field*, *Phys. Scr.* **96**, 095001 (2021).
- [68] P. A. González et al., *Hawking radiation and propagation of massive charged scalar field on a three-dimensional Gödel black hole*, *Gen. Relativ Gravit.* **50**, 62 (2018).
- [69] R. A. Konoplya, *Shadow of a black hole surrounded by dark matter*, *Phys. Lett. B* **795**, 1 (2019).
- [70] S. Vagnozzi and L. Visinelli, *Hunting for extra dimensions in the shadow of M87**, *Phys. Rev. D* **100**, 024020 (2019).
- [71] J. L. Synge, *The escape of photons from gravitationally intense stars*, *Mon. Not. Roy. Astron. Soc.* **131**, (3), 463 (1966).
- [72] J. -P. Luminet, *Image of a spherical black hole with thin accretion disk*, *Astron. Astrophys.* **75**, 228 (1979).
- [73] J. M. Bardeen, *Timelike and null geodesics in the kerr metric*, *Black Holes (Les Astres Occlus)*, pages 215–239. Gordon and Breach, New York, 1973.
- [74] M. A. Anacleto, J. A. V. Campos, F. A. Brito and E. Passos, *Quasinormal modes and shadow of a Schwarzschild black hole with GUP*, *Annals of Physics* **434**, 168662 (2021).
- [75] K. Jusufi, *Black holes surrounded by Einstein clusters as models of dark matter fluid*, [arXiv:2202.00010 \[gr-qc\]](https://arxiv.org/abs/2202.00010)
- [76] K. Jusufi, *Quasinormal Modes of Black Holes Surrounded by Dark Matter and Their Connection with the Shadow Radius*, *Phys. Rev. D* **101**, 084055 (2020).
- [77] Z. Li and C. Bambi, *Measuring the Kerr spin parameter of regular black holes from their shadow*, *JCAP* **1401**, 041 (2014).
- [78] C. Bambi and K. Freese, *Apparent shape of super-spinning black holes*, *Phys. Rev. D* **79**, 043002 (2009).
- [79] G. Gyulchev, P. Nedkova, V. Tinchev and S. Yazadjiev, *On the shadow of rotating traversable wormholes*, *Eur. Phys. J. C* **78** (7), 544 (2018).
- [80] S. Haroon, K. Jusufi and M. Jamil, *Shadow Images of a Rotating Dyonic Black Hole with a Global Monopole Surrounded by Perfect Fluid*, *Universe* **6** (2), 23 (2020).
- [81] A. Belhaj and Y. Sekhmani, *Shadows of rotating quintessential black holes in Einstein–Gauss–Bonnet gravity with a cloud of strings*, *Gen. Relativ Gravit.* **54** (2021).
- [82] D. I. Kazakov and S. N. Solodukhin, *On quantum deformation of the Schwarzschild solution*, *Nuclear Physics B* **429** 1, 153 (1994).
- [83] D. J. Gogoi and U. D. Goswami, *Quasinormal Modes and Hawking Radiation Sparsity of GUP corrected Black Holes in Bumblebee Gravity with Topological Defects*, [arXiv:2203.07594 \[gr-qc\]](https://arxiv.org/abs/2203.07594) (2022).
- [84] V. H. Cárcenas et al., *Probing the parameters of a Schwarzschild black hole surrounded by quintessence and cloud of strings through four standard astrophysical tests*, *EPJC* **81**, 866 (2021).
- [85] J. M. Todelo and V. B. Bezerra, *Black holes with quintessence in pure Lovelock gravity*, *Gen. Relativ. Gravit.* **51**, 41 (2019).
- [86] L. Xiang and X. Q. Wen, *A heuristic analysis of black hole thermodynamics with generalized uncertainty principle*, *JHEP* **10**, 046 (2009).
- [87] R. J. Adler, P. Chen and D. I. Santiago, *The Generalized Uncertainty Principle and Black Hole Remnants*, *Gen. Relativ. Gravit* **33**, 2101 (2001).
- [88] [Official website of LISA](https://www.lisa.nasa.gov/).
- [89] [Official website of ET](https://www.esa.int/ESA/Science_and_Exploration/Space_Science/Event_Horizon_Telescope).